Tellus (2003), 55B, 54–70
Printed in UK. All rights reserved

TELLUS
ISSN 0280–6509

Tropospheric transport of continental tracers towards Antarctica under varying climatic conditions

By G. KRINNER* and C. GENTHON, *Laboratoire de Glaciologie de de Géophysique de l'Environnement, CNRS-UJF, Grenoble, France*

(Manuscript Received 26 November 2001; in final form 11 September 2002)

ABSTRACT

We present a method to analyse tracer transit time climatologies based on the concept of tracer age. The method consists of introducing idealized, short-lived radioactively decaying tracers in a general circulation model of the atmosphere. Tracer age since emission is calculated at any given place in the atmosphere from the ratio of the concentrations of tracers with different lifetimes emitted over the same source area. An obvious use of this method is the analysis of transport of real tracers with similar lifetimes (such as dust particles) during different climatic periods. Here, this method is applied to transport from southern hemisphere continental source areas towards Antarctica at the present, the last glacial maximum (21 kyr BP) and the last glacial inception (115 kyr BP). It is found that the variation over time of atmospheric transport efficiency towards Antarctica depends on the tracer source region: changes for Patagonian tracers differ from those for tracers originating over Australia and southern Africa. Transport towards Antarctica during the last glacial maximum (LGM) is faster for Patagonian, but not for Australian and Southern African tracers. It is shown that for the time of the last glacial inception, tracer transit time towards Antarctica is not significantly different from the present, although signs of a more vigorous atmospheric circulation can be seen in the simulation.

1. Introduction

The problem of tracer transport from low-latitude source regions towards the ice sheets is of interest for several reasons. Ice core analysis yields information about past tracer concentrations (e.g. continental dust, sea salt, etc.) whose variations in time must be interpreted in terms of variations of atmospheric transport towards the ice sheets, and of variations in sources and sinks (Petit et al., 1981). Analysis of atmospheric tracer transport in atmospheric general circulation models (AGCMs) can help explain the observed variations. As variations of tracer concentrations in ice cores over time reflect changes in atmospheric circulation (and therefore climate), the analysis of these variations is a valuable tool for characterizing the different climate states.

Here, we focus on transport of tracers of continental origin towards the Antarctic. Probably the most important type of these tracers is atmospheric dust, due to its (poorly understood) direct and indirect effects on global climate (e.g. Miller and Tegen, 1998; Martin, 1990). Strong variations of dust concentration in polar ice cores (Petit et al., 1999) and marine sediments (Kent, 1982) have been observed between glacials and interglacials, but rapid and strong variations also occur within glacial periods (Petit et al., 1999). Several modelling studies have focused on glacial–interglacial changes in dust deposition in, and/or transport to, polar regions (e.g. Joussaume, 1990; Genthon, 1992; Andersen et al., 1998; Reader et al., 1999; Lunt and Valdes, 2001; Mahowald et al., 1999). Concerning East Antarctica, mineralogical and isotopic studies (Grousset et al., 1992; Basile et al., 1997) indicate that the

*Corresponding author.
e-mail: krinner@lgge.obs.ujf-grenoble.fr
Present address: LGGE, DU BP 96, 38402 St Martin d'Hères Cedex, France.

high glacial dust deposition rates are linked primarily to the Patagonian dust source.

Radon (^{222}Rn) is another tracer of continental origin. This natural radioactive gas, emitted ubiquitously from soils by decay of ^{226}Ra, has a lifetime of 5.5 d and is therefore an interesting tracer of tropospheric transport. It can for example be used in the analysis of events of rapid atmospheric transport to Antarctica (e.g. Wyputta, 1997). An intercomparison of tracer transport models focusing on ^{222}Rn (Jacob et al., 1997) has shown that three-dimensional synoptic models (of the type used in this study) generally do a reasonable job of simulating transport of continental plumes over several days, but the models tend to underestimate ^{222}Rn levels in the upper troposphere. As the sources and sinks of this gas are simple, the interpretation of measured ^{222}Rn concentrations in terms of atmospheric transport is comparatively more straightforward for ^{222}Rn than for continental dust. However, because of the short lifetime of ^{222}Rn, past atmospheric concentrations of this gas are obviously not recorded in ice cores. However, ^{222}Rn-like tracers may nonetheless serve e.g. as a simplified model proxy for dust in the past.

Indeed, in this paper we present an analysis of modelled transport of idealized tracers similar to ^{222}Rn towards Antarctica from continental source regions in South America, Southern Africa and Australia, focussing on transport duration and its variability under different climatic conditions. As we do not simulate existing tracers, simulated and measured tracer concentrations cannot be directly compared. Instead, we focus on the analysis of atmospheric transport (of any short-lived tropospheric tracer: ^{222}Rn, dust etc.) under varying atmospheric conditions, and discuss the model results in the light of knowledge obtained from ice-core records. That is, we address the question of variations in transport efficiency over time, and how these variations of atmospheric transport might be reflected in Antarctic ice core archives. For those readers not familiar with Antarctica, Fig. 1 displays a map of the continent with place names referred to in the text.

We use a direct method of tracer modelling within a GCM as described in the following section. Section 3 presents the characteristics of modelled present-day atmospheric transport towards Antarctica in the polar version of the LMDZ GCM (Krinner et al., 1997). We then present results obtained for the last glacial maximum (21 kyr BP) and for the last glacial inception (115 kyr BP).

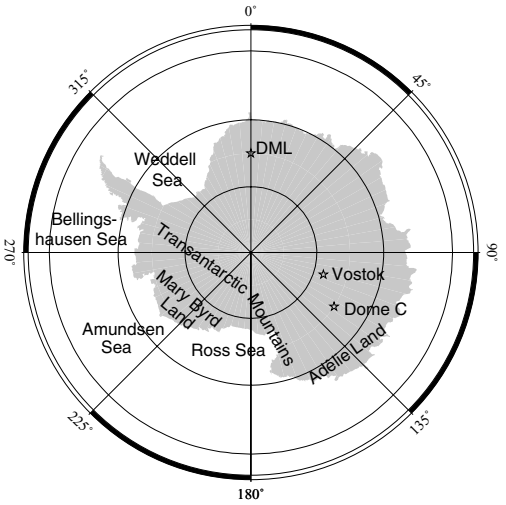

Fig. 1. Map of Antarctica with place names referred to in the text. On this and all following maps, the Greenwich meridian is on top and the 90°E meridian is on the right.

2. Method of tracer transport analysis

The analysis presented below is based on inline eulerian tracer modelling in a general circulation model of the atmosphere. Radon-like tracers with lifetime τ are used. Tracer concentration C is always set to $C_0 = 1$ in the first atmospheric level over a predefined source region S (for example, Patagonia). The tracer is then advected by atmospheric flow out of the source region and decays like radioactive material. Radioactive decay, the only sink here, may be seen as a crude approximation of other removal processes such as gravitational settling, wet removal, etc. Note that setting the tracer concentration to $C_0 = 1$ over the source region is equivalent to imposing a tracer source whose strength varies with (vertical and/or horizontal) wind speed in the first atmospheric layer: in the absence of atmospheric motion near the surface, the effective source strength becomes almost zero, as only the decaying tracer material in the stationary air mass directly above the source is replaced. Conversely, when surface wind speed is high, the tracer source is strong as relatively depleted air is advected over the source area.

The concentration C_τ at a given destination point D (anywhere over the globe) is:

$$C_\tau = C_0 \int_0^\infty \mathrm{f}(t)\mathrm{e}^{-\frac{t}{\tau}}\,\mathrm{d}t, \qquad (1)$$

where $f(t)\Delta t$ gives the fraction of the air mass at D which has been over S in a small time interval Δt at time t in the past (note that time axis is positive backwards). The function $f(t)$ describes the history of atmospheric mixing and advection. The fact that tracer concentration is set to 1 when an air mass reaches the lowest level over a source area means a total loss of memory of the previous history of this air mass. Therefore, $f(t)$ can give no information about the air mass history before that moment.

When two tracers with different lifetimes τ_1 and τ_2 are simultaneously emitted over the same source region, the ratio of their concentrations at D is

$$\frac{C_{\tau_1}}{C_{\tau_2}} = \frac{\int_0^\infty \mathrm{f}(t)\mathrm{e}^{-\frac{t}{\tau_1}}\,\mathrm{d}t}{\int_0^\infty \mathrm{f}(t)\mathrm{e}^{-\frac{t}{\tau_2}}\,\mathrm{d}t}. \tag{2}$$

We know that $\int_0^\infty \mathrm{f}(t)\,\mathrm{d}t \leq 1$ because the concentration C_τ at destination must be lower or equal to the initial concentration C_0, but the exact form of $f(t)$ is unknown. Supposing that the concentration C found at D will be essentially due to a single passage of the air mass over the source region at time t_0 in a not too distant past, $f(t)$ will become similar to a Dirac distribution: $f(t) \approx \delta(t_0)$. In this case, the ratio of the two tracer concentrations at D will simply become

$$\frac{C_{\tau_1}}{C_{\tau_2}} = \frac{\mathrm{e}^{-\frac{t_0}{\tau_1}}}{\mathrm{e}^{-\frac{t_0}{\tau_2}}}, \tag{3}$$

which can be solved for t_0:

$$t_0 = \frac{1}{\frac{1}{\tau_2} - \frac{1}{\tau_1}} \ln\left(\frac{C_{\tau_1}}{C_{\tau_2}}\right) \tag{4}$$

with t_0 indicating the mean tracer age observed at D for tracers with lifetime between τ_1 and τ_2, originating over the source region S. This equation simply reflects the intuitive fact that the concentration ratio of longer-lived vs. shorter-lived species will increase with the length of the atmospheric transport. Taking the limit $\tau_2 \to \tau = \tau_1$ of eq. (4), we obtain:

$$t(\tau) = \lim_{\tau_2 \to \tau} t_0 = \frac{\tau^2}{C_\tau}\frac{\partial C_\tau}{\partial \tau}. \tag{5}$$

We now show that eq. (5) remains valid when air masses are mixed or diluted. Consider mixing of two air masses $i\,(i \in \{1, 2\})$. Suppose that the new resulting air mass is composed of fractions f_i $(\sum_i f_i = 1)$ of the two initial air masses, each with tracer age t_i and tracer concentration C_i. The mean tracer age of the resulting air mass, $\overline{t}$, is simply the weigthed mean of the tracer ages:

$$\overline{t} = \sum_i \left(\frac{f_i C_i}{\overline{C}} t_i\right), \tag{6}$$

with

$$\overline{C} = \sum_i (f_i C_i). \tag{7}$$

On the other hand, eq. (5) would yield

$$\begin{aligned}\overline{t} &= \frac{\tau^2}{\overline{C}}\frac{\partial \overline{C}}{\partial \tau} = \frac{\tau^2}{\overline{C}}\frac{\partial \sum_i (f_i C_i)}{\partial \tau} \\ &= \sum_i \left(\frac{f_i C_i}{\overline{C}}\frac{\tau^2}{C_i}\frac{\partial C_i}{\partial \tau}\right) = \sum_i \left(\frac{f_i C_i}{\overline{C}} t_i\right).\end{aligned} \tag{8}$$

That is, eq. (5) yields the weighted mean of the initial tracer ages [eq. (6)], and therefore remains valid.

The distinction between the age of an air mass and the age of short-lived tracers within an air mass (as defined here) is fundamental. McKeen et al. (1990) and McKeen and Liu (1993) have shown that due to atmospheric mixing, air mass age (in the sense of time since last passage over a defined source area) cannot be correctly estimated from the analysis of concentration ratios of short-lived tracers. In fact, after mixing of two air masses, tracer age (in the sense of mean age of the tracers present in the air mass) following eq. (4) will be lower than the mean age of the two air masses, essentially because the "younger" air mass has a higher tracer content. Actually, the concept of air mass age is frequently used in the analysis of air-mass exchange between the troposphere and the stratosphere (Hall and Plumb, 1994; Eluszkiewicz et al., 2000; Holzer and Hall, 2000). These authors show that air mass age (time since an average air molecule in a given air parcel last passed over a predefined source area) is of the order of several years, depending on the size of the source region S. This is because although some molecules might have passed over D only a short time ago, some "stragglers" may have taken an arbitrarily long atmospheric pathway between S and D (Holzer and Hall, 2000). In our case, tracer age will be limited by the lifetime τ of the tracer: "stragglers" simply decay. Consequently, tracer age t_0 will be of the order of τ, that is, a few weeks at most. However, the tracer age, not the air mass age, is precisely what we are interested in here.

It is important to note that the results obtained here in terms of tracer age depend on the lifetimes of the

tracers used. The interest of the results lies in their relative variations between different climatic periods, yielding information about changes in the characteristics of the atmospheric transport, not in the absolute values. On the other hand, the results are not very sensitive to the size of the source regions.

Characteristics of mean transport of short-lived tracers can therefore easily be analyzed in a GCM when the diagnostic tracers introduced here are used. The mean duration of tracer transport between S and D is calculated as

$$\overline{d} = \frac{1}{\frac{1}{\tau_2} - \frac{1}{\tau_1}} \overline{\ln\left(\frac{C_1}{C_2}\right)} \tag{9}$$

where the overline indicates a time mean.

Statistics of instantaneous values of t_0 [e.g. its time mean $\overline{d}$, given by eq. (9), or short-term, seasonal and interannual variability, etc.] can be used to infer properties of atmospheric transport such as for example frequency of events of particularly fast tracer advection towards Antarctica. This will be done in the following sections for tracers originating in the continents surrounding Antarctica and for different climatic periods [present day, last glacial maximum (21 kyr BP), and last glacial inception (115 kyr BP)].

The simulations are carried out with a tracer version (LMDZ-T) of the LMDZ general circulation model, optimized for polar climate modelling by Krinner et al. (1997). Hourdin and Armengaud (1999) introduced the Van Leer I tracer advection scheme (Van Leer, 1977) into the LMDZ AGCM. They state that in the GCM context, this second-order scheme is an attractive compromise between numerical accuracy and computational expenses. Van Leer I is slightly more diffusive than the Van Leer III advection scheme (Van Leer, 1977), better known to the meteorological community as the slope scheme of Russel and Lerner (1981). However, Hourdin and Armengaud (1999) state that in particular for studies of short-lived tropospheric tracers, the use of a more accurate tracer advection scheme than Van Leer I is not warranted, as processes such as vertical turbulent mixing combined to vertical wind shear also contribute to horizontal tracer diffusion. The GCM is run at regular resolution of 96 $\times$ 72 horizontal grid points and 19 vertical levels. Each simulation spans 5 yr. The source areas are (1) South America polewards of 20°S, (2) Africa south of 10°S and (3) Australia and New Zealand. For each source region, we have two tracers with lifetimes $\tau_1 = 5$ d and $\tau_2 = 10$ d. Tracer ages, calculated after eqs. (4) and (9), will therefore be representative for tracers with an intermediate lifetime (between 5 and 10 d).

3. Present day

3.1. Simulation

The atmospheric GCM is forced by present-day seasonally, but not interannually varying mean sea surface conditions for the years 1979–95. Sea surface temperatures were obtained from 16-yr means of the monthly values used in the AMIP (Gates, 1992) project, while mean sea ice fractions were obtained in the same way using data from National Snow and Ice Data Center (1978–95). The transport of real ^{222}Rn in previous versions of the LMD GCM has been evaluated against observed concentrations by Genthon and Armengaud (1995) and Jacob et al. (1997).

The version of LMDZ used here displays some biases in the modelled atmospheric circulation around Antarctica. In particular, the circumpolar low-pressure belt is too deep and too zonal in winter (Genthon et al., 2002). The impact of these biases on the simulated tracer ages is best assessed by comparing simulated tracer age in the baseline model version to the age calculated in a nudged version of the model (Genthon et al., 2002). Nudging consists in forcing the (simulated) atmospheric circulation in the GCM with observed or analysed atmospheric data. The model is forced at each time step and at three latitudinal bands (40, 50 and 60°S) using temporally interpolated 6-hourly surface pressure, and wind speeds from the ECMWF ERA15 reanalysis dataset (Gibson et al., 1996). Although observational constraint on meteorological analyses is rather weak over the Southern Ocean, the ERA15 reanalyses are considered to be globally one of the best sources of homogeneous long-term atmospheric data, and are widely used for model validation (e.g. Connolley, 1997). In the nudged simulation, the atmospheric circulation between the continental source areas and Antarctica is thus constrained by meteorological analyses which currently provide the best representation of the real state of the global atmosphere. The issue of spurious vertical motions induced by the nudging technique, which could induce unrealistic vertical tracer transport in the model, has been addressed by Genthon et al. (2002) and found of limited importance. Moreover, tracer transport studies have successfully been carried out previously with a nudged version of the LMDZ GCM (Hourdin and

Issartel, 2000). It seems reasonable therefore to suppose that nudged tracer transport on the pathway to Antarctica is also realistic.

3.2. Mean tracer age

3.2.1. Near the surface. Figure 2 displays, for the free (i.e. not nudged) model, the simulated annual mean tracer age for the three continental source regions (the "age" is calculated for the first model level, ≈10 m above the surface). As Patagonia reaches further South than either Africa or Australia/New Zealand, it is not surprising that the tracers from Patagonia arrive much faster than those from the two other source regions, the transport from Africa being the longest. The typical age is about 5.5 d for tracers from Patagonia, 6.5 d for Australian tracers and about 8.5 d for advection from Southern Africa. Interannual variability of mean first-level tracer age is of the order of 2% of the mean age (not shown).

Tracer transport towards the Antarctic is faster in the free model than in the nudged model (not shown), for all three source regions. However, in the interior of Antarctica, the difference is only about 2%, i.e. similar to the interannual variability. On the other hand, over the great West Antarctic embayments (Weddell and Ross Seas), transit time in the free model is up to 5% less than that of the nudged model. In terms of absolute differences, this seems quite low, but as will be shown later, one should take into account that the difference in transit time between present and LGM is only 10%. Apart from errors over the Ross and Weddell Seas, the global patterns in the free and nudged model are very similar, with, for example, fast penetration of Patagonian tracer masses in the Dronning Maud Land (DML) sector. In any case, these model biases have to be kept in mind in the following discussions, which will mostly be limited to the free (i.e. unnudged) model simulation.

3.2.2. Above the inversion layer. One of the most prominent features of the Antarctic climate is the strong, persistent surface temperature inversion (Phillpot and Zillman, 1970; Connolley, 1996). This stable stratification of the atmospheric boundary layer reduces turbulent fluxes between atmosphere and surface and within the boundary layer itself. In particular, the turbulent transfer of atmospheric tracers from the free atmosphere to the surface (and on to the snow) can be inhibited, or at least slowed. It is therefore of interest to study the tracer age difference between the surface and the atmosphere above the inversion layer.

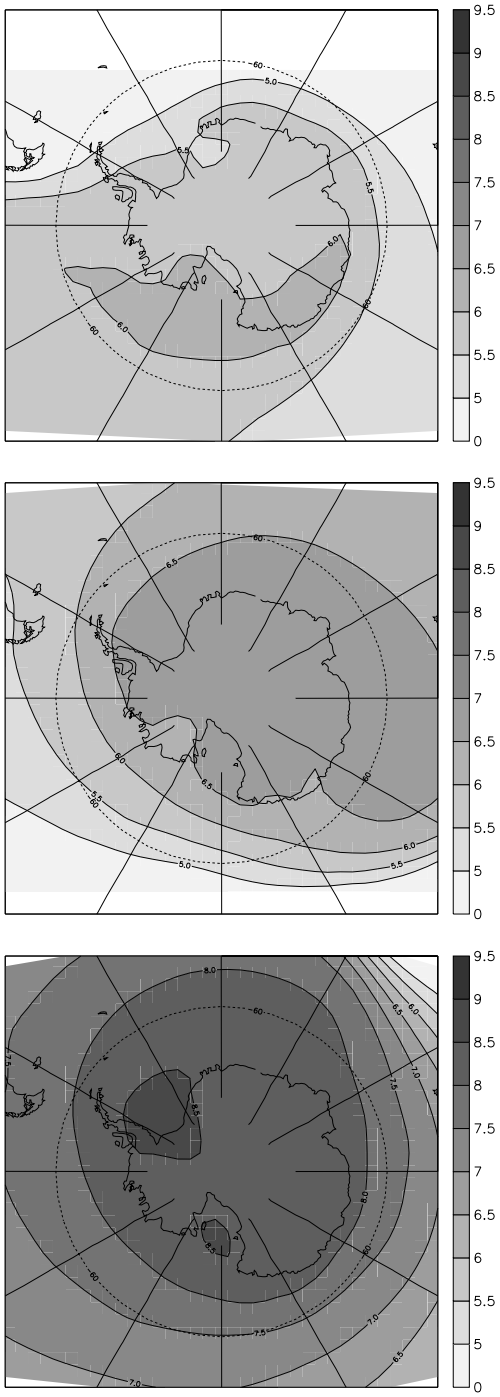

Fig. 2. Simulated mean tracer age (in days) for the present with the free model. Origins are, from top: Patagonia (top), Australia (middle), and Southern Africa (bottom).

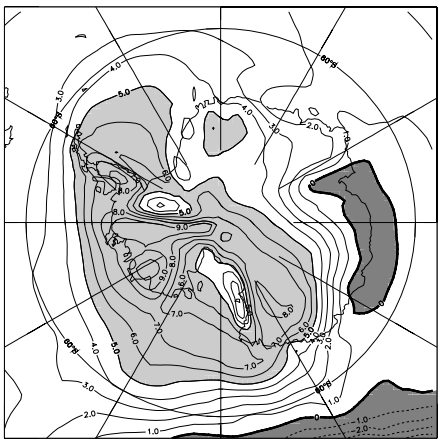

Fig. 3. Relative age difference (in %) for the Australian tracer between 7th model layer (about 1400 m height) and first model layer (about 10 m height), for the present-day simulation. Dark (light) grey: tracers near the surface are younger (more than 5% older) than those aloft.

Typical inversion layer depth in Antarctica, reasonably well reproduced by LMDZ, is several hundreds of metres (Phillpot and Zillman, 1970). Figure 3 displays, for the Australian tracers and the free model run, the relative age difference between the tracers in the seventh model layer (at about 1000 m height over the Antarctic Plateau and 1800 m over the ocean) and the first model layer (at about 10 m above the surface). The patterns of vertical age differences are qualitatively similar (but rotated in longitude, except for terrain-induced features) for Patagonian and South African tracers. In the Pacific sector of Antarctica, first-level Australian tracer age is up to 10% higher than tracer age above the inversion layer. This is broadly the region where the Australian tracer is youngest, consistent with the typically spiral-like east-southeasterly pathways of synoptic systems towards the Antarctic (e.g. Jones and Simmonds, 1993). Tracer transport over the ocean is fastest in the mid-troposphere. When air masses cross the Antarctic coast from the ocean, this happens preferentially at that height. The tracer particles are then slowly (over several hours) transferred to the surface through boundary-layer turbulence, or, particularly further inland, through subsidence (e.g. James, 1989). In the areas that are not subject to fast direct advection of Australian air masses, the age difference between 1 km height and the near-surface air is much less. In particular, near the coast between 60°E and 120°E the Australian tracer is even younger near the surface than aloft. A probable explanation is that this is due to the katabatic wind circulation. These strong near-surface winds lead to stronger turbulent fluxes in the boundary layer, thereby reducing the tracer age difference between surface air and air aloft. In addition, these winds can themselves advect younger tracers along the surface, offsetting the normal tracer cross-boundary layer transit and the subsequent vertical tracer age gradient. Similar structures can be seen over the Transantarctic Mountains and the Ellesworth Range, where the rugged topography increases the modelled turbulent fluxes (Krinner and Genthon, 1998) and strong katabatic winds flowing towards the ice shelves are observed (e.g. Bromwich, 1989).

3.3. *Atmospheric tracer fluxes*

For both present-day simulations, Fig. 4 shows the seasonal cycle of the vertically integrated meridional

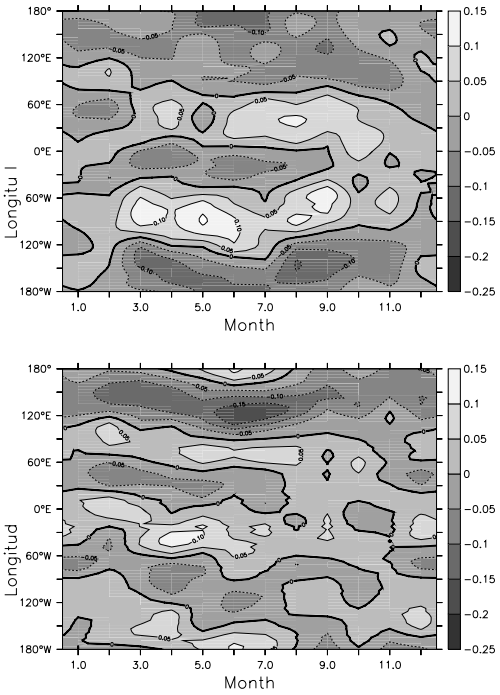

Fig. 4. Present-day seasonal cycle of the vertically integrated northward flux of the tracer with $\tau = 5$ days from Patagonia through the 60°S latitude circle. Top: Free model; bottom: nudged model. Horizonal axis: month of the year; Vertical axis: longitude. Positive values indicate northward flux. Units are arbitrary. For comparison with later figures, the flux is normalized with respect to the annual mean total atmospheric mass of the tracer.

flux for the Patagonian tracer with $\tau = 5$ d across the 60°S latitude circle. Tracer flux is normalized with respect to the total tracer quantity present in the atmosphere. In both simulations, the patterns of the meridional fluxes for the other tracers (both for different source regions and different lifetimes) are very similar to the fluxes of the 5-d Patagonian tracer. Simulated tracer transport towards the Antarctic region essentially occurs at all seasons in the western part of the Australian/Pacific sector (90°E to 120°W), while tracer mass is exported in the Ross–Bellingshausen Sea region. The Weddell Sea region (60°W to 0°) is characterized by tracer influx especially during the winter season, while to the east, in the western Indian Ocean sector, tracer mass leaves the Antarctic region. In general, the magnitude of the tracer flux is higher during the winter months (months 3–9) than during the summer months. During mid-summer (January) the pattern is more complicated, the wave number 2 pattern visible during the rest of the year being replaced by a wave number 4 pattern, but with a weak amplitude. However, this relatively clear picture of the average annual cycle is not so clear for the individual years.

In the nudged model, tracer transport in winter is more clearly organized in a wave number 3 pattern. The large tracer influx region in the Pacific sector seen in the free model is interrupted in the nudged model by northward tracer flux near the dateline. This is coherent with the fact that the free version of LMDZ does not correctly represent the zonal structure of the observed sea level pressure distribution in the southern circumpolar region: the ternary structure of low-pressure cells around Antarctica is replaced by an essentially wave 2 pattern, because the low pressure center in the Bellingshausen/Amundsen seas is not well picked up by the model. The misfit of the free model is smaller in the summer season. During these months, phases of maxima and minima of northward tracer flux are in better agreement in the free and nudged versions than in winter.

The vertical structure of tracer transport in the free model is displayed in Fig. 5. This figure displays quantities for the 5-d Patagonian tracer, but the pictures are qualitatively the same for the other tracers used in this study (and very similar for the nudged simulation). Not surprisingly, westward flux of these short-lived tracers is largest in the middle to upper troposphere at jetstream latitudes. On the other hand, meridional (north–south) flux of the tracers is actually largest quite close to the surface. Tracer flux is southward below 800 hPa

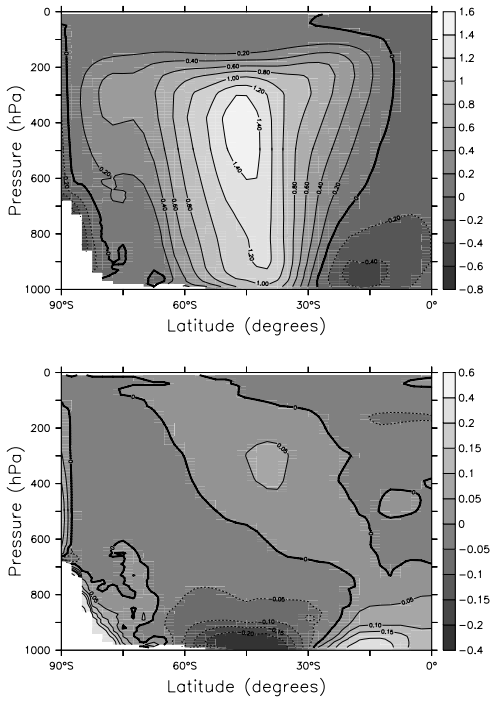

Fig. 5. Annual and zonal mean zonal tracer flux in the free model ($\tau = 5$ days, origin: Patagonia). Top: zonal flux $[\overline{ut}]$, bottom: meridional flux $[\overline{vt}]$. x-axis: latitude (degrees), y-axis: pressure (hPa). Units: arbitrary. Positive values indicate westward flux in the top panel, northward flux in the bottom panel.

between the source region and about 65°S. Polewards of this latitude, the katabatic circulation leads to northward near-surface tracer flux. The general structure of the Antarctic katabatic circulation system, i.e. near-surface drainage flow compensated by southward flux aloft, is reflected by the tracer flux polewards of 65°S.

3.4. Short-term variability

Ice-core records can be affected by extreme events leading for example to unusually fast air mass advection towards the drill site. Such events could for example carry a higher than usual dust load. Dust from these exceptional events would be over-represented in the record (with respect to the temporal frequency of these events), thereby potentially biasing the interpretation of the record (e.g. Tuncel et al., 1989). This general problem of the representativity of core records for the mean climate state has been recognized also for parameters other than dust, such as pollen (e.g. Campbell et al., 1999) or water isotopes (e.g. Jouzel

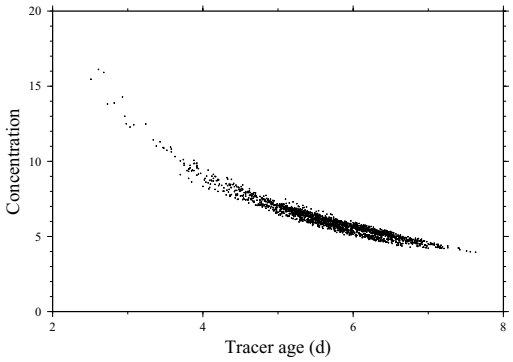

Fig. 6. Scatter-plot of tracer concentration ($\tau = 5$ days, origin: Patagonia) at the EPICA drilling site in Dronning Maud Land, against the advection time from Patagonia. Units: x-axis, days; y-axis: arbitrary.

et al., 1997). Figure 6 illustrates this problem. For each day of the present-day free model simulation, this scatter-plot displays the simulated first-level tracer concentration (Patagonian tracer, $\tau = 5$ d) at the EPICA (European Project for Ice Coring in Antarctica) Dronning Maud Land (DML) drilling site at 75°S and 0°E against the calculated transport time from Patagonia. One can see that low tracer age events are also those that carry quite high tracer concentrations. This is due to two effects. First, faster advection means less tracer decay, and second, it also means relatively little mixing with other, non-Patagonian air masses with lower tracer content. It is therefore of interest to analyze the extrema and the short-term variations of the durations of advection of continental tracers towards Antarctica.

The minimum tracer ages in the nudged simulation (not shown) are quite similar to those of the free model. As events of fast tracer advection should be fairly realistically depicted in the nudged model simulation, this similarity suggests that the free simulation is also likely to capture the types of circulation patterns responsible for fast tracer advection. Therefore, and because the paleoclimate simulations that will be discussed later are of course free (unnudged) simulations, we will focus on the free model simulation in the following.

The 5-yr minimum first-level (10 m) tracer age for the three source regions is shown in Fig. 7. One can see that events of rapid tracer transport towards Antarctica within less than three days occur for tracers from Patagonia and Australia, while African tracers, too far away and well beyond the Antarctic convergence, take

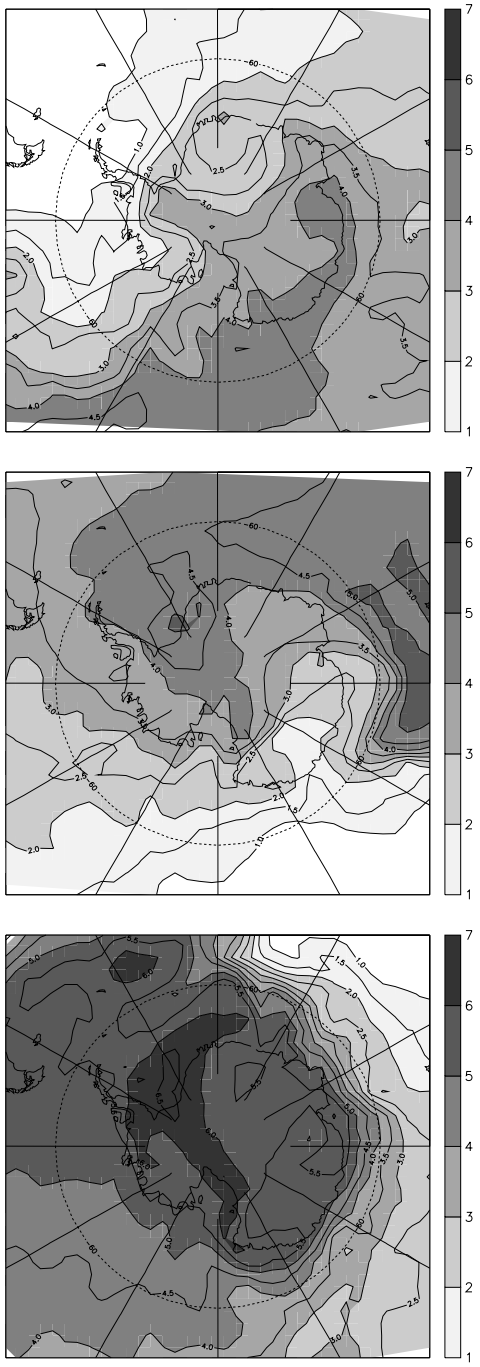

Fig. 7. Simulated minimum tracer age (in days) for the present with the free model. Origins are, from top: Patagonia (top), Australia (middle), and Southern Africa (bottom). Shading interval is one day, contour interval is 0.5 days.

at least 5 d to arrive over Antarctica. Not surprisingly, the "fast" Australian tracers protrude into the interior of Antarctica in Adélie Land, obviously after direct southward flow, while "fast" Patagonian tracers hit the Antarctic continent in Mary Byrd and Dronning Maud Lands. Given the patterns visible in Fig. 7, it is obvious that in these cases, these air masses hit the continent directly from the sea at lower atmospheric levels, and not after advection in the middle troposphere, subsidence over the center of the continent and subsequent northward katabatic flow near the surface, although this is a frequent flow pattern in the Antarctic region (James, 1989). The strong gradient of minimum age of the African tracers along the Indian Ocean sector of the Antarctic coast is in contrast to the smoother distribution for the Patagonian and Australian tracers. As a consequence of the longer transport crossing the Southern Ocean with its strong westerlies, the minimum age distribution for the African tracers is much more zonal than for the other tracers.

Some of the time series of the daily mean values of the simulated tracer ages are displayed in Fig. 8 for the two EPICA sites (Dome C, 75.1°S/123.4°E, and DML, 75.0°S/0.0°E). One can see that the surprisingly low minimum Australian tracer age at Dome C (less than two days) is actually due to one outstanding event, the second fastest event being actually much slower. The situation is different for Patagonian tracers advected towards the EPICA drilling site in Dronning Maud Land, where several fast tracer advection events occurred in the 5-yr simulations. It is difficult to draw very firm conclusions from these facts, because as always with extreme events, it is possible that the picture would be modified if longer simulations were carried out. However, it seems clear that the fastest tracer advection events consistently occur in wintertime, when the atmospheric circulation is much more vigorous than in summer. It is also worth noting that both for Australian and Patagonian air masses, fast air advection events tend to occur almost simultaneously at Dome C and Vostok (not shown). This means that the air masses in these cases generally reach both drilling sites (which is not too surprising, as Dome C and Vostok are only about 600 km apart), generally passing first over Dome C and then over Vostok. However, it is possible that in higher-resolution GCM simulations, this close link between Vostok and Dome would disappear, as air masses could be better separated.

A simple seasonal cycle with relatively fast advection in winter and slower advection in summer can be seen in Fig. 8. Linked to this, the same kind of seasonality can be seen in the tracer amount over the Antarctic region, which is consistently maximum in winter. For the 5-d Patagonian tracer, about 4–5% of the total tracer amount can be found over the Antarctic region (the numbers for the Australian and South African tracers are 3 and 2%, respectively). The seasonal cycle is not so clear for the longer-lived (10 d) tracers. The reason is probably that the winter tracer maximum is due to events of relatively fast air mass advection (Fig. 8), carrying relatively more tracer mass especially for the short-lived tracers.

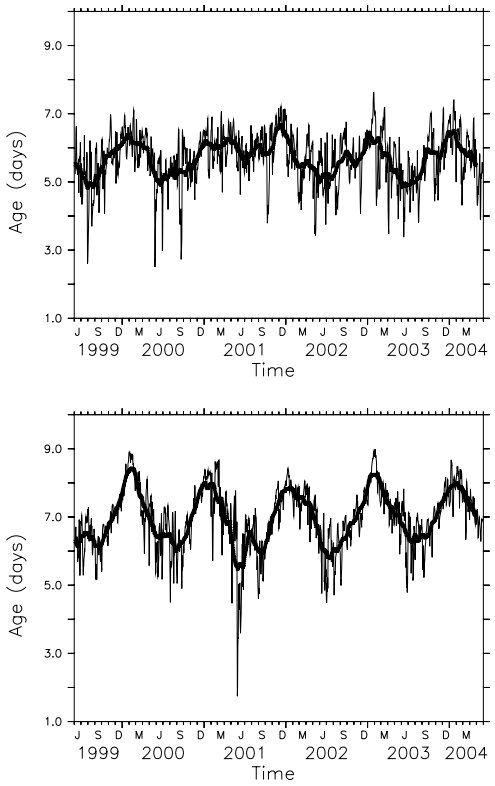

Fig. 8. Time series of the simulated tracer age (days) for the present, at the EPICA deep drilling sites. Top: At Dronning Maud Land for the Patagonian source; Bottom: At Dome C for the Australian source. Thin line: daily values; Thick line: 60-day running mean.

4. Last glacial maximum

4.1. Simulation

The LGM simulation discussed here uses sea surface temperatures and sea-ice extent prescribed after

CLIMAP (1981) except in the North Atlantic, where warmer sea-surface conditions after Weinelt et al. (1996) were imposed on the model. Atmospheric CO_2 concentration was set to 190 ppm, and orbital parameters were modified to LGM values. As in Krinner and Genthon (1998), LGM topography was prescribed following Peltier (1994) except for Greenland, where a topography obtained from glaciological modelling (Ritz et al., 1997) was used. In the following discussion, one has to keep in mind that the CLIMAP (1981) sea-ice extent for the LGM summers in the southern hemisphere is probably too large (Crosta et al., 1998). Characteristics of summer season atmospheric transport as simulated by the model may be affected by this drawback. For a previous version of the LMDZ GCM, the simulated last glacial maximum climate was discussed in detail by Krinner and Genthon (1998).

4.2. Mean tracer age and tracer fluxes

Figure 9 displays the simulated change of the annual mean duration of mean tracer transport from the three continental source regions to the Antarctic surface for the LGM. One can see that the simulated transport for the LGM is up to 10% faster than for the present for the Patagonian tracer, but that, over Antarctica, there is almost no change for the Australian and South African (not shown) tracer age. The fact that the simulated dust transport towards Antarctica is faster for the Patagonian tracer at the LGM than for today in these simulations seems to disagree with other modelling results. For example, Lunt and Valdes (2001) and Reader et al. (1999) report that their models suggest that in terms of tracer concentration, LGM tracer transport from Patagonia towards Antarctica might have been less efficient and conclude that the high observed LGM dust concentrations must have been due to source strength changes. Here, we focus on transit times, which does not reveal strictly the same information as tracer concentration. However, LMDZ also simulates a ≈30% increase of Patagonian tracer loading over the Antarctic at the LGM. More than half of this increase is due to changes in source area (mostly due to the exposed Patagonian continental shelf at the LGM), mean source latitude (the largest part of the additional Patagonian land area at the LGM is located in the southern part of Patagonia, i.e. relatively close to Antarctica, leading to shorter transport) and source strength (an increase in wind speed over these areas results in a stronger source strength, see section 2). The rest of the concentration increase is due to faster transport as a result of changes in the atmospheric circulation patterns (resulting in less tracer loss through radioactive decay before arrival).

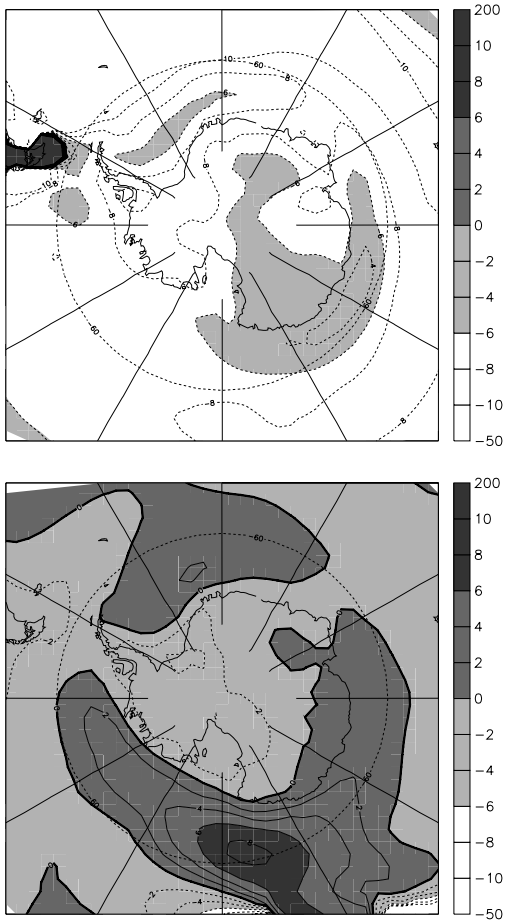

Fig. 9. Simulated change between LGM and present in mean tracer age (in %) for air masses originating in Patagonia (top) and Australia (bottom). Negative values (light shading) indicate younger tracers at the LGM.

The more efficient transport could explain a small fraction of the strong increase in the dust concentrations seen in LGM ice from Antarctic cores (e.g. Petit et al., 1981). Our model result also goes into the right direction in the light of the results of Basile et al. (1997), who have shown that glacial dust in the Vostok core was predominantly of Patagonian origin. Nevertheless it is clear that a 10% decrease in transport time cannot explain a dust concentration increase as strong as the observed one, and that important changes in source strength or atmospheric lifetime are necessary

(e.g. Andersen et al., 1998; Reader et al., 1999; Lunt and Valdes, 2001).

An increased efficiency of atmospheric transport of Patagonian dust during the LGM towards Antarctica has already been simulated in previous versions of the LMDZ GCM (Andersen et al., 1998). In those simulations, the reason for this increase is a simulated increase of the cyclonic activity in the Weddell Sea region (Krinner and Genthon, 1998), favoring particularly southward transport of Patagonian air masses. However, this particular effect is not seen in the simulations presented here. An analysis of the zonal mean of the zonal and meridional tracer fluxes (not shown) shows that an increase in the zonality of the atmospheric circulation during the LGM is clearly visible. Broadly speaking, simulated winds are stronger for the LGM, but it is essentially the zonal wind component that increases, so that the southward transport remains relatively unaffected.

The general structure of the longitudinal distribution of the meridional tracer flux at the LGM (not shown) is fairly similar to the present-day distribution, and therefore not further discussed here.

4.3. Short-term variability

Minimum tracer ages for the LGM are displayed in Fig. 10 for the Patagonian and Australian tracers. Compared to the present-day climate, fast transport from Patagonia occurs well into the heart of Antarctica at the LGM. On the other hand, no such exceptional event as that found in the present climate (section 3.4) can be seen for LGM Australian tracers. However, given the scarcity of such events at the present (one in five years of simulation), this change is not necessarily significant. It is possible that the increased zonality of the atmospheric circulation over the Southern Ocean prevents such events from taking place at the LGM, although we cannot exclude of course that in longer simulations such events could occur. Again, a comparison of Dome C and Vostok time series (not shown) shows that extreme events tend to occur almost simultaneously at the two stations, as stated in section 3.

The time series of daily mean values of tracer age at Vostok, Dome C and the EPICA DML drilling site at the LGM (shown, for the Patagonian tracers at Dome C only, in Fig. 11) all show the same seasonal cycle as already seen for the present (i.e. faster advection in winter). The seasonality of Patagonian tracer age seems slightly more pronounced at the LGM than today. The slight increase in mean transport efficiency of Patagonian air towards Antarctica discussed at the beginning of this section (Fig. 9) is due to faster advection in winter, while in summer the simulated tracer transport times towards Dome C and Vostok do not change much.

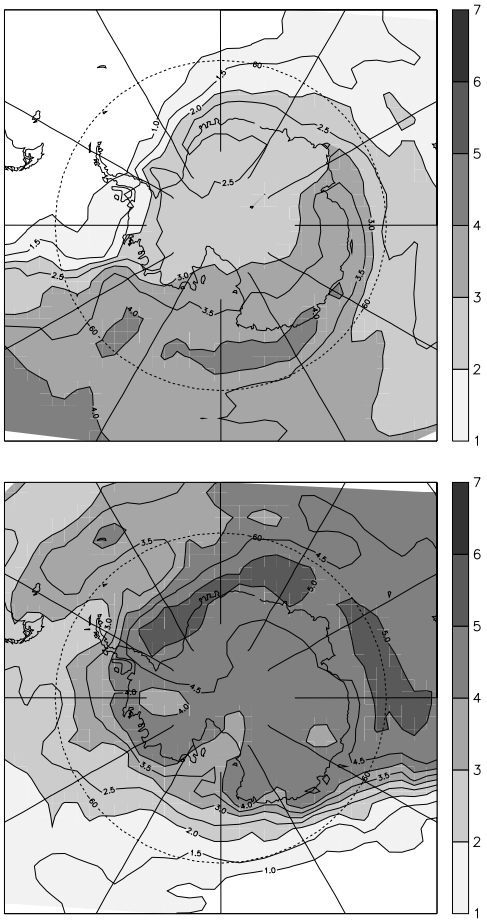

Fig. 10. Simulated LGM 5-year minimum tracer age (in days) for air masses originating in Patagonia (top) and Australia (bottom). Shading interval is one day, contour interval is 0.5 days.

5. Last glacial inception

5.1. Simulation

At the time of glacial inception in the Northern Hemisphere, 115 000 yr ago, the accumulation-corrected concentration of sea salt in the Vostok ice

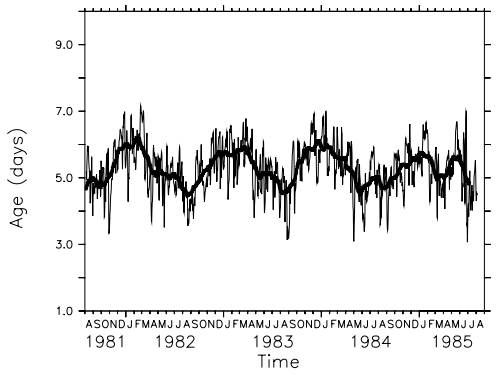

Fig. 11. Time series of the simulated tracer age (days) for the LGM, at the EPICA deep drilling site DML for the Patagonian source. Thin line: daily values; Thick line: 60-day running mean. The years on the x-axis are meaningless.

core (Petit et al., 1999) was roughly twice as high as today, indicating high wind speeds over the Southern Ocean and/or faster air mass advection into the interior of East Antarctica. On the other hand, corrected crustal calcium concentrations were very similar to present-day values, indicating weak changes in sources and atmospheric transport of dust (or, less probably, mutually cancelling changes). The combined evidence from dust and sea-salt makes the last glacial inception circulation in high southern latitudes very intriguing. Differences between the present-day simulation and the run for the last glacial inception (115 kyr BP) are a modified atmospheric CO_2 concentration (280 ppm instead of 330 ppm for the control run) and modified orbital parameters following de Noblet et al. (1996). Sea-surface conditions at high southern latitude sites at 115 kyr BP were suggested to have been about 3 °C cooler than today (Pichon et al., 1992), and the role of the ocean in the initiation of the glaciation in the southern hemisphere was shown to be important (Kim et al., 1998). However, because to our knowledge no global reconstructed SST data set for 115 kyr BP exists, two simulations were carried out. In the first simulation (115WARM), sea surface conditions were not modified compared to the present [similar to GCM studies by de Noblet et al. (1996) and Gallimore and Kutzbach (1996)]. In the second simulation (115COLD), sea surface conditions in the Southern Ocean were modified by latitudinally stretching the observed present-day sea surface temperature between the Antarctic coast and 45°S continously and in such a way that at 60°S, where the deformation is maximum, the new sea surface temperature and sea ice concentration data are actually those observed today at 65°S. This leads to a cooling of a few degrees in the Southern Ocean (with a consistent increase in sea ice cover), in broad agreement with Pichon et al. (1992).

Another possibility would have been to use sea-surface temperatures from a coupled model 115 kyr BP experiment, but the only model output accessible to us (Khodri et al., 2001) does not reproduce very well the present-day observed sea-surface conditions in the Antarctic region, so that using the SST and sea-ice for 115 kyr BP from that model, in a study focussing on the Antarctic region, is not warranted (P. Braconnot, personal communication).

5.2. *Results*

5.2.1. Simulated climate change. Both in 115-WARM and in 115COLD, the model simulates a rather strong summer cooling in boreal continental regions (about −6 °C). This is consistent with the modified orbital forcing which, through a reduced summer insolation in the boreal regions, leads to decreased snow ablation and ultimately, through internal feedback loops, to ice-sheet build-up (e.g. de Noblet et al., 1996; Khodri et al., 2001).

Opposed to this fairly strong change in the northern hemisphere, the simulated climate change over the Antarctic region is rather weak, even in 115COLD. At Vostok, 115 kyr BP mean annual surface temperatures are colder than today by only 2 °C in 115COLD, while they are almost the same as today in 115WARM. Isotope analysis of the ice core drilled at that site indicates that the climate at 115 kyr BP was about 4 °C cooler than today (Petit et al., 1999). Thus it seems that the (prescribed) cooling over the Southern Ocean in 115COLD is not sufficient to force strong cooling over Antarctica. The cooling at Vostok in 115COLD is strongest in winter (−4 °C) and rather weak in summer. As shown by Krinner and Genthon (1998), this is due to the fact that the polar climate is particularly sensitive to surface temperatures of the surrounding oceans during the cold season, when, due to the quasi-absence of solar radiation, the only heat source is warm air advection from lower latitudes. In summer, the presence of solar radiation diminishes the relative importance of warm air advection in the heat budget. The annual mean cooling over the Southern Ocean in 115COLD is essentially limited to the lower troposphere below 5000 m, whereas a warming is visible at the same latitudes above 8000 m (Fig. 12). Limitation of the

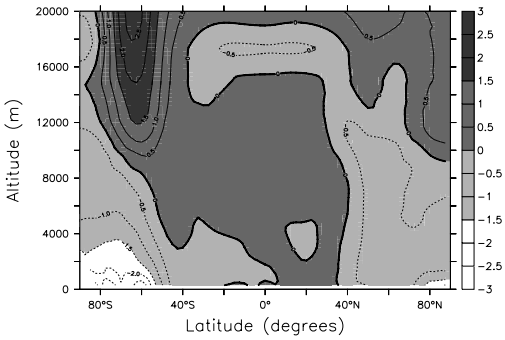

Fig. 12. Simulated annual and zonal mean temperature difference (in °C) between 115COLD and the present-day free simulation. Horizontal axis: Latitude (degrees); Vertical axis: Altitude (m).

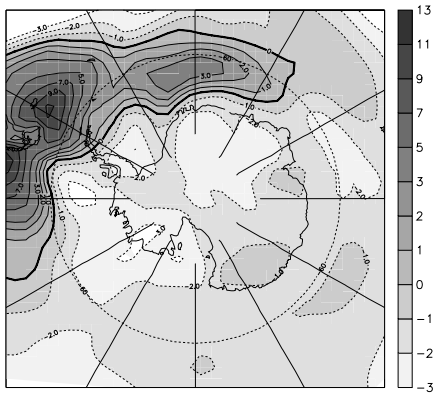

Fig. 13. Relative tracer concentration difference in surface air (in %) between 115COLD and the present-day free simulation for the 5-day Patagonian tracer. Negative values mean lower concentrations in 115COLD.

cooling to the levels below 500 hPa (≈5000 m in these latitudes) is not surprising. For example, Simmonds and Budd (1991) report that the warming caused by removal of the Antarctic sea ice is limited to atmospheric levels below 500 hPa. The warming above 8000 m is related to the colder SST over the Southern Ocean. Like the the near-surface cooling, it is not seen in 115WARM. The reason for the warming in the upper troposphere is not clear to us. Annual mean westerly wind speed over the Southern Ocean in 115COLD is increased throughout the troposphere, by 1 m s^{-1} at the surface up to several m s^{-1} near the tropopause (not shown). In 115WARM, no such changes are visible.

5.2.2. Impact on tracer ages, concentrations and fluxes. For both 115 kyr BP simulations the simulated mean tracer age for the three source areas at the last glacial inception (not shown) is not significantly different from the present-day values. Given the relatively weak difference in the simulated climate between 115 kyr BP and today (compared to the large changes between the LGM and today), and given the fact that already for the LGM, the simulated tracer ages are quite close to those for the present, it is not surprising that the mean tracer ages for 115 kyr BP and the present are very similar. Mean tracer concentrations at 115 kyr BP are slightly lower than today by about 2% (115COLD) and 3% (115WARM) as can be seen in Fig. 13 for the 5-d Patagonian tracer in 115COLD (numbers are similar for the other tracers). Simulated interannual variability of surface air concentration of this tracer is about 4% in the interior of Antarctica (not shown). Therefore, this signal is not statistically significant at a high confidence level. On the other hand, tracer concentrations at 115 kyr BP are lower than the simulated present-day values in both 115 kyr BP simulations and, systematically, for all six tracers. This makes us confident that this signal is meaningful, although the different tracers in one GCM run are not totally independent between each other. This is particularly true for any pair of tracers from the same source region, as they tend to be influenced by the same meteorological events. Conversely, the tracer concentration change, both in 115COLD and 115WARM (Fig. 13), shows an increase of tracer mass over the Southern Ocean, in particular downwind of the source area, and a decrease over Antarctica. This points towards the beginning of a relative climatic isolation of Antarctica from the lower latitudes, and thus from its heat sources over the Southern Ocean, at 115 kyr BP.

Ice core analysis (e.g. Petit et al., 1999) shows, if anything, a small increase in the crustal dust concentration at 115 kyr BP compared to the preceeding interglacial. The simulations here rather suggest that atmospheric transport towards Antarctica might have been less efficient at 115 kyr BP than it is at the present interglacial. However, source effects and impacts of climate change on dust deposition rates are not represented in the simulations discussed here. These effects could easily account for the misfit. On the other hand, the observed increase of sea salt in Antarctic ice at 115 kyr BP seems to be in agreement with the more vigorous atmospheric circulation when colder SST are prescribed (simulation 115COLD). Although the rather weak climate change between 115 kyr BP

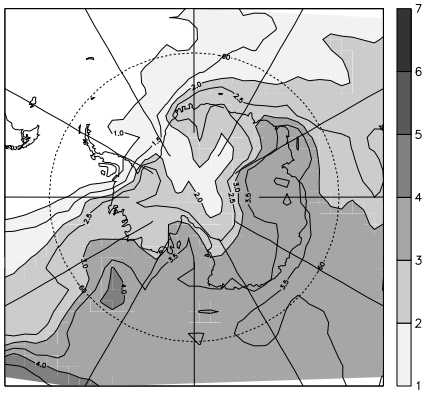

Fig. 14. Simulated minimum age of the 5-day Patagonian tracer in 115COLD (in days). Shading interval is one day, contour interval is 0.5 days.

and today does not modify mean tracer age in Antarctica, it does seem to have an impact on rapid tracer advection events. Figure 14 displays the minimum age of the 5-d Patagonian tracer in simulations 115COLD. One can see that the minimum age is clearly lower than what can be seen for the present (Fig. 7). A similar effect is also seen in 115WARM and in tracer age time series for both 115 kyr BP simulations (not shown). The air mass transport at the time of glacial inception at 115 kyr BP therefore seems to be in a sense intermediate between the present and the LGM.

6. A note on ice-core sampling

In an ice core, one can only measure the mean concentrations $\overline{C_i}$ of the idealized tracers discussed here over a given time period. The length of this period would be determined for example by the instrumental resolution (at least a month or so, more generally a season or a year). The mean duration $\overline{d}$ of the transport [given in eq. (9)] would therefore have to be estimated by

$$\overline{d} = \frac{1}{\frac{1}{\tau_2} - \frac{1}{\tau_1}} \ln\left(\frac{\overline{C_1}}{\overline{C_2}}\right). \tag{10}$$

This would of course only be possible if these kind of "ideal" tracers existed in reality, if their removal process described by the lifetime τ was only active in the atmosphere (the concentration being frozen once the tracer touches ground over the ice sheet), and if the air–snow transfer function were perfectly known. This discussion is not as unrealistic as it may sound, as for example changes in dust particle size spectra can be used to deduce qualitative informations about changes in atmospheric circulation patterns (Petit et al., 1990), using the fact that larger dust particles have shorter atmospheric lifetimes than smaller ones. It is therefore of interest to note that the mean tracer age [eq. (9)] and its ice-core proxy [eq. (10)] have almost identical values for the simulations presented here, that is, both for the present and past climates. This means that for tracers with lifetimes similar to those used here, for example atmospheric dust of appropriate particle size, interpretation of relative tracer mass variations in terms of tracer age does not seem to be seriously affected by sampling as illustrated by eqs. (9) and (10).

7. Conclusion

The tracer method presented here can give valuable insight into the effects of climate change on the transport of atmospheric tracers. Its strength (and weakness) resides in the fact that it is based on idealized tracers. This is an advantage, as effects of variations of source and sink strength are not to be considered. It is a disadvantage, as direct comparisons with measured tracer concentrations are not possible. The method presented here allows a simple analysis of a key parameter in the interpretation of concentrations of short-lived tracers (e.g. dust) in ice cores: the age of the tracer in surface air over the ice sheet. In this context one may note that, in particular in regions where katabatic winds are strong, tracer presence in the first model layer (at about 10 m height) does not necessarily mean high tracer deposition rates at the surface. However, the drill sites discussed in more detail in this work (Vostok, DML and Dome C) are not located in areas known for strong winds.

The method presented here gives information about tracer age, as opposed to air mass age. That is, the results one obtains are modulated by the prescribed lifetime of the tracers. This is an advantage, as the information one gets out of it is actually closer to what one finds in an ice core (even with idealized tracers), but it is a disadvantage in the sense that no absolute (that is, tracer-independent) information is given about the characteristics of the atmospheric circulation. We note that this drawback could be eliminated by introducing a larger number of tracers of this kind with different lifetimes τ, yielding a tracer age spectrum $t(\tau)$ [see eq. (5)] as a function of tracer lifetime.

This spectrum then contains more complete information about atmospheric transport characteristics. This improvement would of course have a computational cost. However, it is worth noting here that, compared to model runs without passive tracers, the additional numerical cost of running the GCM with six tracers, as done in this study, is about 20%. This is actually fairly reasonable.

An interesting alternative method of studying atmospheric transport of trace species has been presented by Hourdin et al. (1999). This method basically consists of time-reversed off-line eulerian tracer modelling. Whereas the lagrangian back-tracking only accounts for large-scale transport, the approach by Hourdin et al. (1999), based on time symmetry of the transport equations, can also be applied to other transport processes such as turbulent mixing. However, this method suffers from the same inconvenience as the back-trajectory technique, that is it requires high-frequency storage of three-dimensional wind and other fields. In short, the method presented here and other existing methods have both advantages and drawbacks. The use of this or any other method of analysis of atmospheric transport must depend on the exact nature of the information one hopes to obtain.

Applying the method presented here to simulations of present and past climates shows that, in agreement with paleo-data, atmospheric tracer transport from Patagonia to East Antarctica might have been more efficient at the LGM, in particular in winter, but not enough to explain alone the observed dust concentrations at the LGM. On the other hand, advection of tracers from other continental regions in the Southern Hemisphere does not seem to have been favoured during the glacial. At 115 kyr BP, which corresponds to the last glacial inception, atmospheric transport towards Antarctica shows signs of a more vigorous circumpolar circulation, but the effect on tracer age and Antarctic near-surface concentrations is negligible. This seems coherent with the analysis of dust and sea salt in the Vostok ice core (Petit et al., 1999), which suggests the onset of a more rigorous atmospheric circulation over the Southern Ocean at that time, but no significant increase in tracer concentrations.

8. Acknowledgments

This work is a contribution to the "European Project for Ice Coring in Antarctica" (EPICA), a joint ESF (European Science Foundation)/EC scientific programme, funded by the European Commission and by national contributions from Belgium, Denmark, France, Germany, Italy, the Netherlands, Norway, Sweden, Switzerland and the United Kingdom. This is EPICA publication no. 50. We also thank the French *Programme National de l'Etude de la Dynamique du Climat* for support.

REFERENCES

Andersen, K., Armengaud, A. and Genthon, C. 1998. Atmospheric dust under glacial and interglacial conditions. *Geophys. Res. Lett.* **25**, 2281–2284.

Basile, I., Grousset, F., Revel, M., Petit, J.-R., Biscaya, P. and Barkov, N. 1997. Patagonian origin of glacial dust deposited in East Antarctica (Vostok and Dome C) during glacial stages 2, 4 and 6. *Earth Planet. Sci. Lett.* **146**, 573–589.

Bromwich, D. 1989. Satellite analyses of katabatic wind behavior. *Bull. Am. Meteorol. Soc.* **70**, 738–749.

Campbell, I., McDonald, K., Flannigan, M. and Kringayark, J. 1999. Long-distance transport of pollen into the Arctic. *Nature* **399**, 29–30.

CLIMAP, 1981. *Seasonal reconstructions of the Earth's surface at the last glacial maximum*, volume MC-36 of, *Geol. Soc. Am. Map Chart Ser.* Geol. Soc. Am.

Connolley, W. 1996. The Antarctic temperature inversion. *Int. J. Climatol.* **16**, 1333–1342.

Connolley, W. 1997. Variability in annual mean circulation in high southern latitudes. *Clim. Dynam.* **13**, 745–756.

Crosta, X., Pichon, J. and Burckle, L. 1998. Reappraisal of Antarctic seasonal sea-ice at the Last Glacial Maximum. *Geophys. Res. Lett.* **25**, 2703–2706.

de Noblet, N., Prentice, C., Joussaume, S., Texier, D., Botta, A. and Haxeltine, A. 1996. Possible role of atmosphere–biosphere interactions in triggering the last glaciation. *Geophys. Res. Lett.* **23**, 3191–3194.

Eluszkiewicz, J., Hemler, R., Mahlman, J., Bruhwiler, L. and Takacs, L. 2000. Sensitivity of age-of-air calculations to the choice of advection scheme. *J. Atmos. Sci.* **57**, 3185–3201.

Gallimore, R. and Kutzbach, J. 1996. Role of orbitally induced changes in tundra area in the onset of glaciation. *Nature* **381**, 503–505.

Gates, W. 1992. AMIP: the atmospheric model intercomparison project. *Bull. Am. Meteorol. Soc.* **73**, 1962–1970.

Genthon, C. 1992. Simulations of desert dust and sea salt aerosols in Antarctica with a general circulation model of the atmosphere. *Tellus* **44B**, 371–389.

Genthon, C. and Armengaud, A. 1995. Radon 222 as a comparative tracer of transport and mixing in two general

circulation models of the atmosphere. *J. Geophys. Res.* **100**, 2849–2866.

Genthon, C., Krinner, G. and Cosme, E. 2002. Free and laterally-nudged Antarctic climate of an Atmospheric General Circulation Model. *Monthly Weather Rev.* **130**, 1601–1616.

Gibson, R., Kållberg, P. and Uppala, S. 1996. The ECMWF re-analysis (ERA) project. *ECMWF Newsletter* **73**, 7–16.

Grousset, F., Biscaye, P., Revel, M., Petit, J.-R., Pye, K., Joussaume, S. and Jouzel, J. 1992. Antarctic (Dome C) ice-core dust at 18 ky BP: Isotopic constraints on origins. *Earth Planet. Sci. Lett.* **111**, 175–182.

Hall, T. and Plumb, R. 1994. Age as a diagnostic of stratospheric transport. *J. Geophys. Res.* **99**, 1059–1070.

Holzer, M. and Hall, T. 2000. Transit-time and tracer-age distributions in geophysical fluids. *J. Atmos. Sci.* **57**, 3539–3558.

Hourdin, F. and Armengaud, A. 1999. The use of finite-volume methods for atmospheric advection of trace species. part I: Test of various formulations in a general circulation model. *Mon. Wea. Rev.* **127**, 822–837.

Hourdin, F. and Issartel, J.-P. 2000. Sub-surface nuclear test monitoring through the CTBT xenon network. *Geophys. Res. Lett.* **27**, 2245–2248.

Hourdin, F., Issartel, J.-P., Cabrit, B. and Idelkadi, A. 1999. Reciprocity of atmospheric transport of trace species. *C. R. Acad. Sci. Paris* **329**, 623–628.

Jacob, D., Prather, M. and 28 co-authors, 1997. Evaluation and intercomparison of global atmospheric transport models using ^{222}Rn and other short-lived tracers. *J. Geophys. Res.* **102**, 5953–5970.

James, I. N. 1989. The Antarctic drainage flow: implications for hemispheric flow on the Southern hemisphere. *Antarctic Sci.* **1**, 279–290.

Jones, D. A. and Simmonds, I. 1993. A climatology of southern hemisphere extratropical cyclones. *Clim. Dynam.* **9**, 131–145.

Joussaume, S. 1990. Three-dimensional simulations od the atmospheric cycle of desert dust particles using a general circulation model. *J. Geophys. Res.* **95**, 1909–1941.

Jouzel, J., Alley, R., Cuffey, K., Dansgaard, W., Grootes, P., Hoffmann, G., Johnsen, S., Koster, R., Peel, D., Shumann, C., Stievenard, M. and White, J. 1997. Validity of the temperature reconstruction from water isotopes in ice cores. *J. Geophys. Res.* **102**, 26471–26488.

Kent, D. 1982. Apparent correlation of paleomagnetic intensity and climatic records in deep-sea sediments. *Nature* **299**, 538–539.

Khodri, M., Leclainche, Y., Braconnot, P., Marti, O. and Cortijo, E. 2001. Simulating the amplification of orbital forcing by ocean feedbacks in the last glaciation. *Nature* **410**, 570–574.

Kim, S.-J., Crowley, T. and Stössel, A. 1998. Local orbital forcing of Antarctic climate change dur last interglacial. *Science* **280**, 728–730.

Krinner, G. and Genthon, C. 1998. GCM simulations of the Last Glacial Maximum surface climate of Greenland and Antarctica. *Clim. Dynam.* **14**, 741–758.

Krinner, G., Genthon, C., Li, Z.-X. and Le Van, P. 1997. Studies of the Antarctic climate with a stretched-grid general circulation model. *J. Geophys. Res.* **102**, 13731–13745.

Lunt, D. and Valdes, P. 2001. Dust transport to Dome C ice core, Antarctica, at the Last Glacial Maximum and present day. *Geophys. Res. Lett.* **28**, 53–56.

Mahowald, N., Kohfeld, K., Hansson, M., Balkanski, S., Harrison, Y., Prentic, I., Schulz, M. and Rodhe, H. 1999. Dust sources and deposition during the Last Glacial Maximum and current climate: A comparison of mode lresults with paleodata from ice cores and marine sediments. *J. Geophys. Res.* **104**, 15895–15916.

Martin, J. 1990. Glacial–interglacial CO_2 change: the iron hypothesis. *Paleoceanography* **5**, 1–13.

McKeen, S. and Liu, S. 1993. Hydrocarbon rations and photochemical history of air masses. *Geophys. Res. Lett.* **20**, 2363–2366.

McKeen, S., Trainer, M., Hsie, E., Tallamraju, R. and Liu, S. 1990. On the direct determination of atmospheric OH radical concentrations from reactive hydrocarbon measurements. *J. Geophys. Res.* **95**, 7493–7500.

Miller, R. and Tegen, I. 1998. Climate response to soil dust aerosols. *J. Climate* **11**, 3247–3267.

National Snow and Ice Data Center. Northern hemisphere weekly snow cover and sea ice extent, 1978–95. Digital data availabe from nsidc@kryos.colorado.edu.

Peltier, W. R. 1994. Ice age paleotopography. *Science* **265**, 195–201.

Petit, J.-R., Briat, M. and Royer, A. 1981. Ice age aerosol content from East Antarctic ice core samples and past wind strength. *Nature* **293**, 391–394.

Petit, J.-R., Jouzel, J., Raynaud, D., Barnola, J.-M., Basile, I., Bender, M., Chappellaz, J., Davis, M., Delaygue, G., Delmotte, M., Kotlyakov, V., Legrand, M., Lipenkov, V., Lorius, C., Pépin, L., Ritz, C., Saltzman, E. and Stievenard, M. 1999. Climate and atmospheric history of the past 420 000 years from the Vostok ice core, Antarctica. *Nature* **399**, 429–436.

Petit, J.-R., Mounier, L., Jouzel, J., Korotkevich, Y., Kotlyakov, V. and Lorius, C. 1990. Paleoclimatological implications of the Vostok core dust record. *Nature* **343**, 56–58.

Phillpot, H. R. and Zillman, J. W. 1970. The surface temperature inversion over the Antarctic continent. *J. Geophys. Res.* **75**, 4161–4169.

Pichon, J., Labeyrie, L., Bareille, G., Labracherie, M., Duprat, J. and Jouzel, J. 1992. Surface water temperature changes in the high latitudes of the Southern Hemisphere over the last glacial-interglacial cycle. *Paleoceanogr.* **7**, 289–318.

Reader, M., Fung, I. and McFarlane, N. 1999. The mineral dust aerosol cycle during the Last Glacial Maximum. *J. Geophys. Res.* **104**, 9381–9398.

Ritz, C., Fabre, A. and Letréguilly, A. 1997. Sensitivity of a Greenland ice sheet model to ice flow and ablation parameters: consequences for the evolution through the last climatic cycle. *Clim. Dynam.* **13**, 11–24.

Russel, G. and Lerner, J. 1981. A new finite-differencing scheme for the tracer transport equation. *J. Appl. Meteorol.* **20**, 1483–1498.

Simmonds, I. and Budd, W. 1991. Sensitivity of the southern hemisphere circulation to leads in the Antarctic pack ice. *Q. J. R. Meteorol. Soc.* **117**, 1003–1024.

Tuncel, G., Aras, N. and Zoller, W. 1989. Temporal variations and sources of elements in the South Pole atmosphere. 1. Nonenriched and moderately enriched elements. *J. Geophys. Res.* **94**, 13025–13038.

Van Leer, B. 1977. Towards the ultimate conservative difference scheme. part IV: A new aproach to numerical convection. *J. Comput. Phys.* **23**, 276–299.

Weinelt, M., Sarnthein, M., Pflaumann, U., Schultz, H., Jung, S. and Erlenkeuser, H. 1996. Ice-free nordic seas during the last glacial maximum? Potential sites of deepwater formation. *Paleoclimates* **1**, 283–309.

Wyputta, U. 1997. On the transport of trace elements into Antarctica using measurements at the Georg-von-Neumayer station. *Tellus* **49B**, 93–111.